CHARACTERISTICS OF MOISTURE PATHWAYS ASSOCIATED WITH LARGE PRECIPITATION EVENTS IN THE UPPER COLORADO RIVER BASIN

Johnathan P. Kirk[1] and Thomas W. Schmidlin[2]

EXTENDED ABSTRACT

Declining streamflow in mountain snowpack-sourced basins across the western United States in recent years has necessitated further investigation into the spatiotemporal trends of snowpack accumulation each season. Previous studies have shown that substantial proportions of annual precipitation occur during relatively few large precipitation events (LPEs) and consequently, such events tend to be significant predictors of streamflow for many basins, including the Upper Colorado River Basin (UCRB) (McCabe, 1996; Werner & Yeager, 2013; Bolinger et al., 2014). While primary pathways of atmospheric moisture from the Pacific Ocean into the inland interior have been identified in previous studies (e.g. Rutz et al., 2015), comparatively little analysis has been done to examine the moisture pathways associated with LPEs at the watershed-level amid the interior west.

In this study, to analyze moisture pathways associated with LPEs in the UCRB, as a means of ultimately exploring potential water supply forecasting improvements, a synoptic classification of moisture transport was constructed utilizing the self-organizing maps (SOM) procedure (Kohonen, 1995; Hewitson & Crane, 2002). Integrated Vapor Transport (IVT) is often used to represent moisture transport and is calculated as the vertical integration of the product of specific humidity and vector wind velocity across given layers of atmosphere. A recent synoptic classification of IVT utilizing the SOM procedure for analyzing extreme precipitation events across the western United States provides a useful precedent for configuring the classification used in this study, as well as comparing the results of the classifications (Swales et al., 2016).

The results of the synoptic classification produced in this study are shown in Figure 1. Daily IVT data were acquired via the ECMWF (European Centre for Medium-Range Weather Forecasts) ERA-Interim reanalysis dataset at 6-hour time steps for all October-April days from water years 1981-2014 across a spatial domain of 20-55°N and 100-140°W (Dee et al., 2011). Standardized anomalies of IVT were then calculated using running 30-day means and

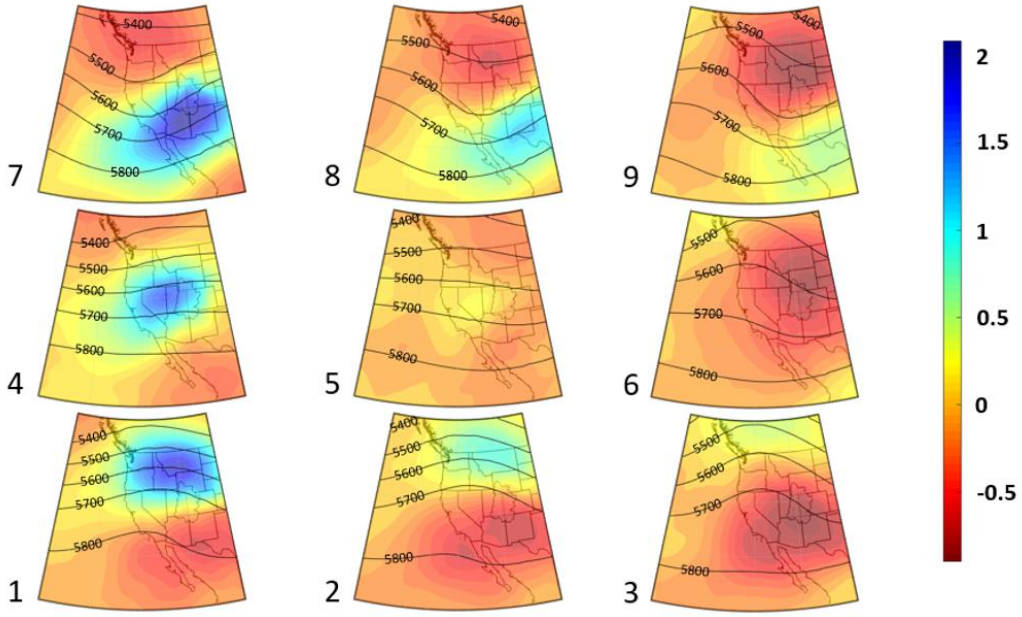

Figure 1. Daily patterns of standardized IVT anomalies (shaded) resulting from the SOM classification procedure, overlaid with 500-hPa geopotential height composites (contours) measured in geopotential meters.

Paper presented Western Snow Conference 2017
[1] Johnathan P. Kirk, Department of Geography, Kent State University, Kent, OH, jkirk9@kent.edu
[2] Thomas W. Schmidlin, Department of Geography, Kent State University, Kent, OH, tschmidl@kent.edu

standard deviations at each grid point. IVT is much larger over ocean than land, so to trace inland moisture transport, the SOM procedure was run for a smaller domain closer to land (30-49°N; 100-118°W), with the results then mapped to the original spatial domain for fuller geographic context, similar to the approach in Swales et al. (2016). Multiple SOM configurations were tested, but ultimately a classification featuring 9 total clusters (3x3 SOM node dimensions) was determined to effectively stratify standardized IVT anomalies while also optimizing the ratio of between-cluster variability to within-cluster variability (Davies & Bouldin, 1979).

As in the classification featured in Swales et al. (2016), positive standardized IVT anomalies are stratified across three latitudinal corridors in conjunction with the corresponding 500-hPa flow regimes. Patterns 1, 4, and 7 show the strongest positive anomalies centered towards the north of the UCRB, aimed at the center of the UCRB, and over southern portions of the UCRB, respectively. The standardized IVT anomalies generally decrease when moving from left to right across Figure 1. Pattern 7 depicts a deep trough just west of the UCRB, suggesting moisture advection from the southwest coinciding with positive vorticity advection east of the trough axis. Interannual variability in this pattern, along with Pattern 8, shows statistically significant positive correlations ($p < 0.05$) to streamflow as measured at United States Geological Survey (USGS) river gages located throughout the UCRB. The magnitudes of the standardized IVT anomalies are not as strong in Patterns 1 and 4, but are still widely positive near and upwind of the UCRB, with flow regimes orienting onshore moisture transport at slightly different latitudes relative to the basin. Patterns 1 and 4 have weak positive correlations to streamflow in the northernmost reaches of the UCRB. Patterns 3, 6, and 9 depict widespread negative standardized IVT anomalies, suggesting dry conditions in the UCRB, broadly coinciding with ridging aloft. Pattern 3 shows the strongest connection to streamflow, with significant negative correlations in interannual variability noted throughout the basin.

To examine air flow during large precipitation events, an air mass climatology during LPEs was constructed based on back trajectories calculated using the Air Resources Laboratory's Hybrid Single Particle Lagrangian Integrated Trajectory model (HYSPLIT) (Draxler & Hess, 1997; Stein et al., 2015). A catalog of LPEs was assembled at 15 snow telemetry (SNOTEL) sites representing five headwater subbasins (drained by USGS river gages) distributed across the UCRB, as defined in Kirk & Schmidlin (2016). Daily precipitation increments observed at each SNOTEL site were calculated and ranked for all days in the period of study. The 80th percentile of the daily precipitation increments was selected as the LPE threshold and captures ~55% of total precipitation. This LPE definition corresponds to 7.6-12.7 mm (0.3-0.5 in) of daily precipitation, which is within the range of large events as defined in prior studies (e.g. Bolinger et al., 2014).

72-hour back trajectories terminating at 18 UTC on all LPE days observed in the UCRB were calculated in HYSPLIT for gridpoints representing each of the sample headwater subbasins. Each trajectory terminates at 500 m above ground level, an elevation roughly at cloud level during LPEs. Trajectories are calculated using North

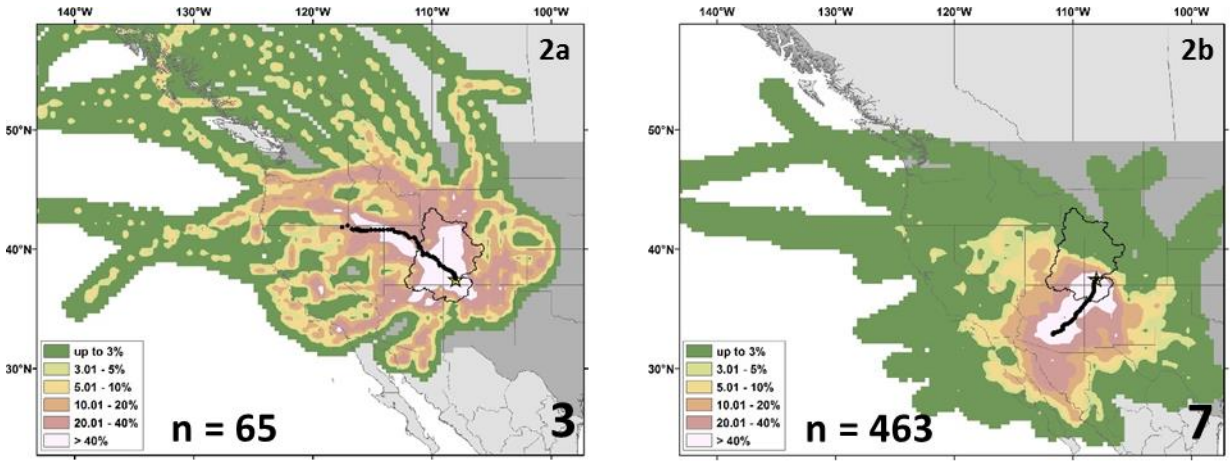

Figure 2. Frequency analyses of back trajectories terminating on LPE days near the Animas River at Durango, CO USGS river gage. Figure 2a (left) depicts the trajectories terminating on LPE days classified as Pattern 3 (dry pattern) in the synoptic classification (shown in Figure 1). Figure 2b (right) represents the trajectories terminating on LPE days classified as Pattern 7 (wet pattern) in the synoptic classification. The sample size (n) of trajectories included in each frequency analysis is also given. The median trajectory is shown in black dots.

American Regional Reanalysis (NARR) meteorological input data (Mesinger et al., 2006). The NARR data represent the highest spatiotemporal resolution dataset that spans the period of study and have been made compatible for use in HYSPLIT calculations. Once back trajectories for each LPE have been calculated, a frequency analysis is created to visualize the trajectories in aggregate, to aid in identifying common corridors of air mass propagation preceding LPEs in the UCRB (Figure 2). The frequency analyses were calculated following a method similar to that described in Hondula et al. (2010).

The trajectory frequencies shown in Figure 2 represent the proportion of all back trajectories passing through a 0.5° latitude/longitude grid as they converge towards the gridpoint representing a headwater subbasin, in this case the Animas River at Durango, CO USGS river gage site (at which point the proportion of trajectories equals 100%). Figure 2a illustrates the trajectories of the air masses leading into LPE days which are classified as Pattern 3 days by the synoptic classification used in this study. Pattern 3 is a dry pattern, with ridging aloft. As such, only 65 LPE days (3.8% of total) are classified as Pattern 3 days. The frequency analysis reveals that many of these air masses curve in from the north and west, around the ridge axis depicted for Pattern 3 in Figure 1. By contrast, Figure 2b shows the trajectories leading into Pattern 7 LPE days. Pattern 7 is characterized by highly positive standardized IVT anomalies and a deep trough. 463 LPE days (27.4% of total) are classified as Pattern 7, the most common of the SOM patterns for LPE days. The frequency analysis illustrates a pronounced southerly to southwesterly flow associated with these LPEs. In general, Patterns 8 and 9 are also characterized by southwesterly flow, Patterns 4-6 have westerly onshore flow, and Patterns 1 and 2 also depict westerly flow, with even lesser contributions from the south/southwest corridor. Similar trajectories by SOM pattern are also noted for the other headwater subbasins.

Through implementing a synoptic classification and an air mass climatology, this study demonstrates how moisture transport can be assessed for the Upper Colorado River Basin and how large precipitation events clearly exhibit preferred atmospheric characteristics. Moisture consolidates into corridors as it infiltrates into the continental interior, with moisture mainly originating from the Pacific Ocean. Large precipitation events in the UCRB most frequently occur during periods of southwesterly flow regimes, in conjunction with trough patterns aloft, but can also occur during zonal flow patterns, particularly in the northern subbasins. The results shown in this study suggest that certain midtropospheric flow regimes are commonly connected to the occurrence of LPEs in the basin. Troughs facilitate moisture advection from the southwest, while ridges often deflect storm tracks away from the UCRB. The occurrence of LPEs has been shown to be a significant predictor of streamflow in the UCRB, therefore, increasingly frequent and/or amplified meridional flow regimes will likely contribute to increased interannual variability in LPE occurrence and streamflow variability in the region. Given these relationships, improved forecasting of long-range midtropospheric flow regimes could offer signals for predicting end-of-season water supply. (KEYWORDS: large precipitation events, synoptic climatology, Colorado River, drought)

REFERENCES

Bolinger, R.A., C.D. Kummerow, and N.J. Doesken. 2014. Attribution and characteristics of wet and dry seasons in the upper Colorado River Basin. *Journal of Climate, 27,* 8661-8673. doi:10.1175/JCLI-D-13-00618.1.

Davies, D.L. and D.W. Bouldin. 1979. A cluster separation measure. *IEEE Transactions on Pattern Analysis and Machine Intelligence, PAMI-1,* 224-227. doi:10.1109/TPAMI.1979.4766909.

Dee, D.P., S.M. Uppala, A.J. Simmons, and Coauthors. 2011. The ERA-Interim reanalysis: configuration and performance of the data assimilation system. *Quarterly Journal of the Royal Meteorological Society, 137,* 553-597. doi:10.1002/qj.828.

Draxler, R. R. and G.D. Hess. 1997. Description of the HYSPLIT_4 modeling system. NOAA Technical Memorandum ERL ARL-224.

Hewitson, B.C. and R.G. Crane. 2002. Self-organizing maps: applications to synoptic climatology. *Climate Research, 22,* 13-26, doi:10.3354/cr022013.

Hondula, D.M., L. Sitka, R.E. Davis, and Coauthors. 2010. A back-trajectory and air mass climatology for the Northern Shenandoah Valley, USA. *International Journal of Climatology, 30,* 569-581. doi:10.1002/joc.1896.

Kirk, J. P. and T.W. Schmidlin. 2016. Defining large precipitation events in the Upper Colorado River Basin and the contributions to Lake Powell inflow. *Proceedings of the 73rd Eastern Snow Conference*.

Kohonen, T. 1995. *Self-Organizing Maps*. Springer-Verlag Berlin Heidelberg. 362 pp.

McCabe, G. J. 1996. Effects of winter atmospheric circulation on temporal and spatial variability in annual streamflow in the western United States. *Hydrological Sciences Journal, 41,* 873-887. doi:10.1080/02626669609491556.

Mesinger, F., G. DiMego, E. Kalnay, and Coauthors. 2006. North American Regional Reanalysis. *Bulletin of the American Meteorological Society, 87,* 343-360. doi:10.1175/BAMS-87-3-343.

Rutz, J.J., W.J. Steenburgh, and F.M. Ralph. 2015. The inland penetration of atmospheric rivers over Western North America: a lagrangian analysis. *Monthly Weather Review, 143,* 1924-1943. doi:10.1175/MWR-D-14-00288.1.

Stein, A.F., R.R. Draxler, G.D. Rolph, and Coauthors. 2015. NOAA's HYSPLIT atmospheric transport and dispersion modeling system. *Bulletin of the American Meteorological Society, 12,* 2059-2077. doi:10.1175/BAMS-D-14-00110.1.

Swales, D., M. Alexander, and M. Hughes. 2016. Examining moisture pathways and extreme precipitation in the U.S. Intermountain West using self-organizing maps. *Geophysical Research Letters, 43,* 1727-1735. doi:10.1002/2015GL067478.

Werner, K. and K. Yeager. 2013. Challenges in forecasting the 2011 runoff season in the Colorado Basin. *Journal of Hydrometeorology, 14,* 1364-1371. doi:10.1175/JHM-D-12-055.1.